Instability of Flow Magnetic Nozzle

Hunt Feng

June 9, 2023

Contents

Abstract

Spectral theory is a common technique for analyzing the instability of a dynamical system. By discretizing the linearized equations motion of magnetic nozzle, the instability problem becomes an algebraic eigenvalue problem. Given Dirichlet boundary condition, we found that the flow in magnetic nozzle is stable. Different discretizations, such as finite difference, finite element and spectral element method agree with each other. By studying the convergence of different modes, we successfully eliminated the spurious unstable modes occur in supersonic and transonic cases.

Chapter 1

Introduction

1.1 Plasma

In this thesis we study the instability of plasma flow in magnetic mirror configuration. We start the thesis by introducing the concept of plasma.

Plasma is one of the four fundamental states of matter, along with solids, liquids, and gases. It is often referred to as the fourth state of matter. Plasma is an ionized gas that consists of highly energized particles, including positively charged ions and negatively charged electrons.

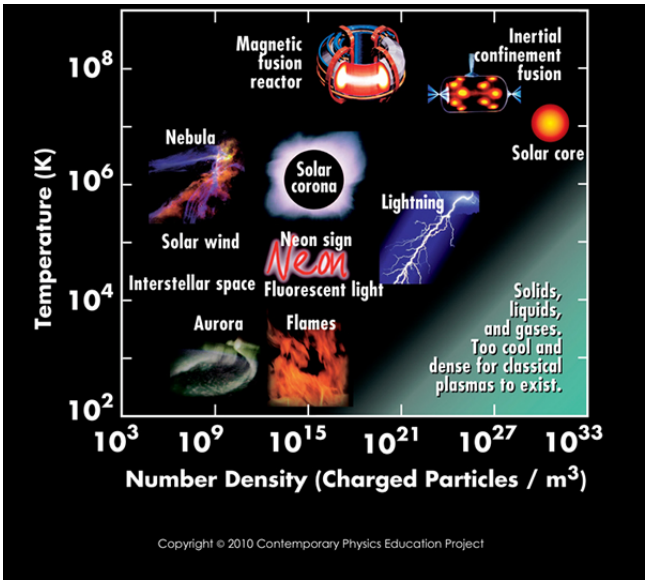

Figure 1.1: Characteristics of typical plasmas.

In a plasma, the atoms or molecules have been stripped of their electrons,

resulting in a collection of charged particles. This ionization process occurs when a gas is subjected to extremely high temperatures or strong electromagnetic fields, which supply sufficient energy to overcome the electrostatic forces that hold electrons in their orbits around atomic nuclei.

Plasma is known for its unique properties. It is an excellent conductor of electricity and is strongly influenced by electromagnetic fields. Plasma also emits light, and examples of natural plasma include stars, such as our Sun, and lightning. Artificially generated plasma can be found in fluorescent lights, plasma televisions, and certain types of industrial torches.

In addition to these applications, plasma has various scientific and technological uses. It is used in plasma physics research, nuclear fusion experiments, plasma cutting and welding, plasma medicine for treating diseases, and even in spacecraft propulsion systems.

Overall, plasma is an intriguing and versatile state of matter with significant implications in various fields of science, technology, and industry.

1.1.1 Single Particle Motion Along Magnetic Field Line

Since plasma consists of charged particles, its motion can is governed by Lorentz force. The equation of motion of a charged particle in magnetic field is given by

$$m\frac{\mathrm{d}\mathbf{v}}{\mathrm{d}t} = q\mathbf{v}\times\mathbf{B}$$

where m is the mass of charged particle, and q is the charge of particles.

Consider a magnetic field pointing in z-direction, $\mathbf{B} = B\hat{\mathbf{z}}$. Since the magnetic force is perpendicular to both $\mathbf{v}$ and $\mathbf{B}$, we can separate the equation of motion into two directions,

$$q\mathbf{v}_\perp\times\mathbf{B} = \frac{mv_\perp^2}{r}\hat{\mathbf{r}}, \quad \mathbf{v}_\parallel = v_\parallel\hat{\mathbf{z}}$$

where $\mathbf{v}_\perp$ is the velocity perpendicular to the magnetic field, and $\mathbf{v}_\parallel$ is the velocity parallel to the magnetic field. In this way, we see that the charged particle gyrates about the magnetic field, doing helical motion along the magnetic field line.

1.1.2 From Kinetic Theory to Fluid Description

In kinetic theory, the charged particles in plasma obey a certain distribution function $f(\mathbf{x},\mathbf{v},t)$. This distribution function is affected by plasma temperature. Assuming there is only one species of particles in the plasma, the plasma temperature is just the sum of the kinetic energy of all particles. We expect at higher temperature, faster the particles will be.

Suppose a collisionless plasma is at equilibrium, then the particles can be characterized by Maxwell-Boltzmann distribution

$$f_M(\mathbf{x},\mathbf{v},t) = \frac{1}{(\pi v_{th}^2)^{3/2}}\exp\left(-\left(\frac{v}{v_{th}}\right)^2\right)$$

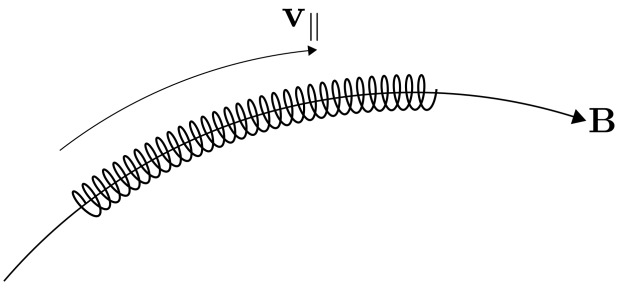

Figure 1.2: A charged particle gyrates about the magnetic field line. The velocity along the field line is $\mathbf{v}_{\parallel}$ and the gyrate frequency, radius is given by the radial equation, $q\mathbf{v}_{\perp} \times \mathbf{B} = \hat{\mathbf{r}} m v_{\perp}^2 / r$. Moreover, for static, nonuniform magnetic field, the charged particle will stay on the same of magnetic field line as it gyrates.

where $v_{th} = \sqrt{2k_B T/m}$ is the thermal velocity.

The moments of the distribution function are suitable macroscopic properties of the plasma. For example, the plasma density and plasma momentum can be viewed as

$$n(\mathbf{x}, t) = \int_{\mathbb{R}^3} f(\mathbf{x}, \mathbf{v}, t) d^3\mathbf{v}$$

$$n\mathbf{V}(\mathbf{x}, t) = \int_{\mathbb{R}^3} \mathbf{v} f(\mathbf{x}, \mathbf{v}, t) d^3\mathbf{v}$$

where $\mathbf{V}$ is the fluid velocity of the charged particle. It is the bulk velocity of the plasma. In magnetic nozzle, since the charged particles flow along the magnetic field line, it is intuitive to think of $\mathbf{V}$ as the plasma flow velocity along the magnetic field line.

In fusion device and space propulsion system, we want high plasma temperature to achieve good performance. Hence, we assume high plasma temperature in this thesis. In other words, the plasma is collisionless.

The distribution function f in a collisionless plasma satisfies the so-called collisionless Vlasov equation, $\mathrm{d}/\mathrm{d}t\ f(\mathbf{x}, \mathbf{v}, t) = 0$. Expand it explicitly, it is

$$\frac{\partial f}{\partial t} + \mathbf{v}\frac{\partial f}{\partial \mathbf{x}} + \frac{q}{m}(\mathbf{E} + \mathbf{v} \times \mathbf{B})\frac{\partial f}{\partial \mathbf{v}} = 0 \tag{1.1}$$

where $q(\mathbf{E} + \mathbf{v} \times \mathbf{B})$ is the Lorentz force experience by the species, the collision term $C(f)$ is dropped. Worth to mention that the electric field and magnetic field are generated by the configuration and the motion of the charged particles.

Integrate both sides with respect to volume element in velocity space, $d^3\mathbf{v}$, we get the conservation of density.

$$\frac{\partial \rho}{\partial t} + \boldsymbol{\nabla} \cdot (\rho \mathbf{V}) = 0$$

If we multiply $\mathbf{v}$ on both sides and integrate with respect to $d^3\mathbf{v}$, we get the conservation of momentum.

$$\rho\frac{\partial \mathbf{V}}{\partial t} + \mathbf{V}\cdot\boldsymbol{\nabla}\mathbf{V} = \frac{q}{m}(\mathbf{E} + \mathbf{V}\times\mathbf{B}) - \boldsymbol{\nabla}p$$

In the process we assume isotropic pressure, and no viscosity exists in the plasma.

As we can see the fluid description only depends on the macroscopic properties of plasma, such as the fluid velocity along the magnetic field line $\mathbf{V}$, density ρ, and pressure p of the plasma. This simplifies the problem.

1.2 Magnetic Nozzle

In this thesis, we are going to deal with plasma flow in magnetic nozzle. A magnetic nozzle is a device that uses a magnetic field to shape and control the flow of charged particles in a plasma propulsion system, see Fig.1.3 . By employing magnetic mirrors, the magnetic nozzle can efficiently direct and accelerate the plasma particles, generating thrust for propulsion. The magnetic field in the nozzle helps collimate and focus the plasma exhaust, increasing its velocity and enhancing the performance of the propulsion system.

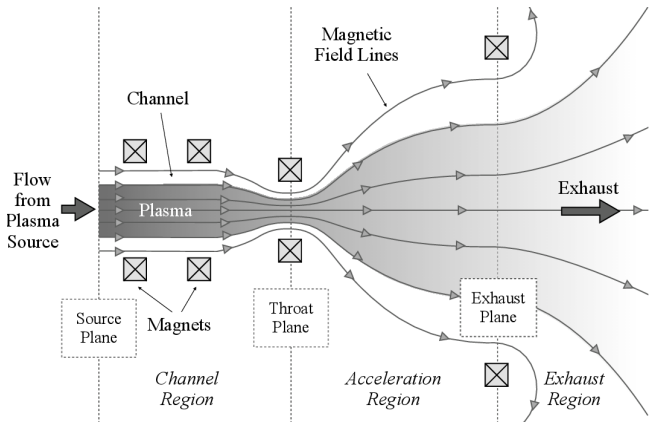

Figure 1.3: Example of a magnetic nozzle configuration. In our models, we define the magnetic nozzle as the region downstream from the throat plane, which can be further divided into an acceleration region and exhaust region. The channel connects the plasma source (not shown) with the magnetic nozzle. [6]

1.2.1 Magnetic Field in Magnetic Nozzle

This thesis will treat the flow in magnetic nozzle as a 1D motion. Hence, the magnetic field can be modeled as

$$B(z) = B_0 \left[1 + R \exp\left(-\left(\frac{x}{\delta}\right)^2\right)\right]$$

where $1 + R$ is the magnetic mirror ratio, it is the ratio of the magnitude of magnetic field at the center of the nozzle to that at the end of the nozzle. Higher the magnetic mirror ratio, larger the difference between the magnitude of magnetic field at the center and at the end. On the other hand, δ determines the spread of the magnetic field. Larger the δ, flatter the magnetic field.

An example of magnetic field is shown in Fig.(1.4).

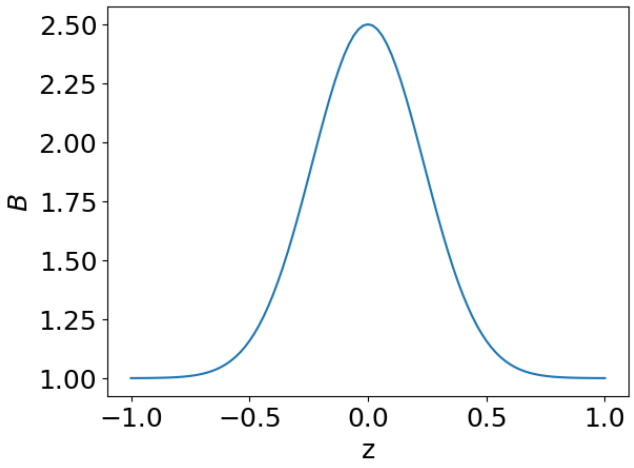

Figure 1.4: This is the magnetic field in nozzle with mirror ratio $1 + R = B_{max}/B_{min} = 2.5$, and the spread of magnetic field, $\delta = 0.1/0.3 = 0.\bar{3}$.

1.2.2 Velocity Profile at Equilibrium

Let n_0 and v_0 be the density and velocity at equilibrium, we know that $\partial n_0/\partial t = 0$ and $\partial v_0/\partial t = 0$ for the solution is stationary, in other words time independent. Therefore n_0 and v_0 satisfy the so-called equilibrium condition,

$$\frac{\partial}{\partial z}\left(\frac{n_0 v_0}{B}\right) = 0$$
$$v_0 \frac{\partial v_0}{\partial z} = -c_s^2 \frac{1}{n_0}\frac{\partial n_0}{\partial z}$$

Let $M(z) = v_0(z)/c_s$ be the mach number (nondimensionalized velocity).

The equations of motion become

$$B\frac{\partial}{\partial z}\left(\frac{n_0 M}{B}\right) = 0$$
$$M\frac{\partial M}{\partial z} = -\frac{1}{n_0}\frac{\partial n_0}{\partial z}$$

Substitute $\frac{1}{n_0}\,\partial n_0/\partial z$ using first equation, the conservation of momentum becomes

$$(M^2-1)\frac{\partial M}{\partial z} = -\frac{M}{B}\frac{\partial B}{\partial z}$$

Notice that there is a singularity at $M = 1$, the sonic speed.

This is a separable equation, integrate it and use the conditions at midpoint $B(0) = B_m, M(0) = M_m$ we get

$$M^2 e^{-M^2} = \frac{B^2}{B_m^2} M_m^2 e^{-M_m^2}$$

We can now express M using the Lambert W function,

$$M(z) = \left[-W_k\left(-\frac{B(z)^2}{B_m^2} M_m^2 e^{-M_m^2}\right)\right]^{1/2}$$

where the subscript k of W stands for branch of Lambert W function. When $k = 0$, it is the subsonic branch; When $k = -1$, it is the supersonic branch. Below shows a few cases of the solution.

- $M_m < 1, k = 0$, subsonic velocity profile.
- $M_m = 1$, $k = 0$ for $x < 0$ and $k = -1$ for $x > 0$, accelerating profile
- $M_m = 1$, $k = -1$ for $x < 0$ and $k = 0$ for $x > 0$, decelerating profile
- $M_m > 1, k = -1$, supersonic velocity profile

Fig.(1.5) shows some cases of the solution.

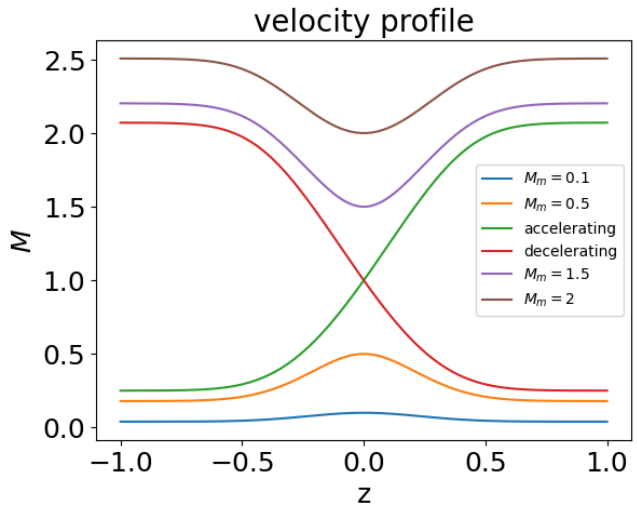

Figure 1.5: The velocity profile in the magnetic nozzle is completely determined by M_m, the velocity at the midpoint, $z = 0$. For the transonic velocity profiles, M_m alone is not enough to determine the profile, we need to specify the branch of Lambert W function to determine whether it is accelerating or decelerating.

1.2.3 Flow in Similar Configuration: Bondi-Parker Flow

Bondi derived a steady-state solution for accretion flow which is governed by Bernoulli's equation in sperical symmetry around a point mass in 1952. Then Parker solved a similar problem but with outward wind in 1958. [1, 2, 5] The equilibrium velocity profiles in such configuration are shown in Fig.1.6.

Solar wind is an example of Bondi-Parker flow. The solar wind is a stream of charged particles, primarily electrons and protons, flowing outward from the Sun.

In summary, the magnetic mirror configuration is a technique that uses magnetic fields to confine and control charged particles. It finds applications in plasma propulsion systems through the use of a magnetic nozzle. Moreover, the solar wind is another example of flows in magnetic mirror configuration. Its acceleration machanism is similar to that of magnetic nozzle.

1.3 Instability of Plasma Flow

1.3.1 Overview

In this section, plasma instability will be introduced and from that we will discuss the importance of this research.

The instability of plasma flow refers to the tendency of a plasma system to deviate from a stable, equilibrium state and exhibit perturbations or fluctua-

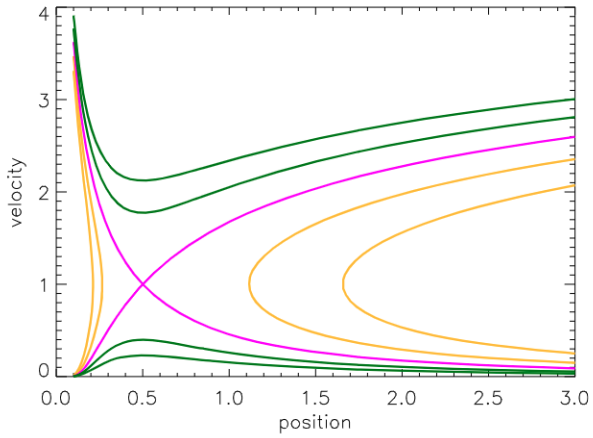

Figure 1.6: Representative trajectories of the steady-state BP flow in non-dimensional units. [5] The upward pink line represents a outward wind, it accelerates from subsonic to supersonic. The downward pink line represents an accretion flow, it accelerates towards the mass point. The green lines below the pink lines represent subsonic flows, and the green lines above represent supersonic flows. Orange lines are physically impossible scenarios.

tions in its behavior. These instabilities can arise from various factors, such as the interaction of particles with electromagnetic fields, collective effects, or the presence of gradients in plasma parameters.

Understanding and studying plasma instabilities are crucial for several reasons:

1. Energy Transport: Plasma instabilities can play a significant role in the transport of energy within a plasma system. They can enhance or hinder the transfer of energy between particles, affecting the overall efficiency and behavior of plasma devices. By studying these instabilities, scientists and engineers can gain insights into the mechanisms governing energy transport in plasmas and develop strategies to control and mitigate them.

2. Plasma Confinement: In applications such as magnetic confinement fusion, achieving and maintaining a high degree of plasma confinement is essential for sustained fusion reactions. Instabilities can lead to the loss of plasma particles, reduction in confinement time, and decreased overall plasma performance. By understanding the nature of these instabilities, researchers can design improved confinement strategies and develop techniques to suppress or stabilize them.

3. Plasma Heating: Instabilities can also influence the heating mechanisms in a plasma system. For example, in magnetic fusion devices, instabilities like the ion temperature gradient (ITG) or electron temperature gradient

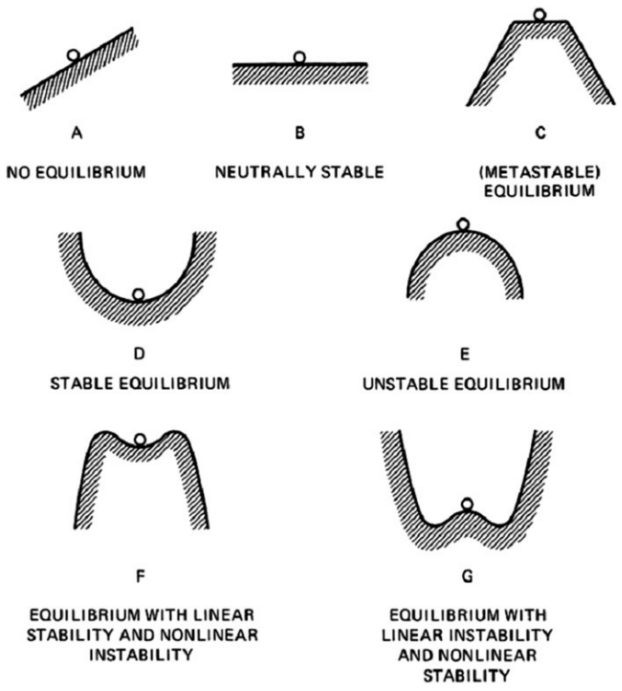

Figure 1.7: Mechanical analogy of various types of equilibrium. [3]

(ETG) instabilities can hinder efficient heating of the plasma. Understanding these instabilities helps in optimizing heating schemes and improving the overall heating efficiency of plasmas.

4. Plasma Diagnostics: Instabilities can manifest as measurable fluctuations in plasma parameters such as density, temperature, and electromagnetic fields. By studying these fluctuations and their characteristics, scientists can employ diagnostic techniques to gain valuable information about the plasma state, identify the presence of instabilities, and assess the stability and health of plasma devices.

1.3.2 Illustration: Two-Stream Instability

We take the famous two-stream instability as an illustration. Let the plasma be cold ($k_B T_e = k_B T_i = 0$), let there be no magnetic field ($B_0 = 0$). The linearized continuity equations are

$$\frac{\partial n_{i1}}{\partial t} + n_0 \frac{\partial v_{i1}}{\partial x} = 0 \tag{1.2}$$

$$\frac{\partial n_{e1}}{\partial t} + n_0 \frac{\partial v_{e1}}{\partial x} + v0 \frac{\partial n_{e1}}{\partial x} = 0 \tag{1.3}$$

And the linearized equations of motion are

$$M n_0 \frac{\partial v_{i1}}{\partial t} = e n_0 E_1 \tag{1.4}$$

$$m n_0 \left(\frac{\partial v_{e1}}{\partial t} + v_0 \frac{\partial v_{e1}}{\partial x} \right) = -e n_0 E_1 \tag{1.5}$$

Here v_0 is the velocity of electron respect to the ions (the ion velocity at equilibrium is taken to be $v_{i0} = 0$), n_0 is the equilibrium density of both ion and electron, v_{i1} and v_{e1} are perturbed velocity of ions and electrons, and E_1 is the perturbed electron field.

If we assume perturbed electric field takes the wave form

$$E_1 = E \exp(i(kx - \omega t))$$

Plug this perturbed electric field into Eq.(1.4) and (1.5), then we can solve for v_{i1} and v_{e1},

$$v_{i1} = \frac{ie}{M\omega} E$$

$$v_{e1} = -\frac{ie}{m} \frac{E}{\omega - k v_0}$$

Using the perturbed velocities, the continuity equations Eq.(1.2) and (1.3) yields

$$n_{i1} = \frac{i e n_0 k}{M\omega^2} E$$

$$n_{e1} = \frac{i e k n_0}{m(\omega - k v_0)^2} E$$

Finally, plug them into the Poisson's equation

$$\epsilon_0 \frac{\partial E_1}{\partial x} = e(n_{i1} - n_{e1})$$

We now have the dispersion relation

$$1 = \omega_p^2 \left[\frac{m/M}{\omega^2} + \frac{1}{(\omega - kv_0)^2} \right]$$

Solving this equation for ω, there is chance we will get complex frequency,

$$\omega = \omega_r + i\omega_i$$

where $\omega_r, \omega_i \in \mathbb{R}$. Then the perturbed electric field becomes

$$E_1 = E \exp(i(kx - \omega_r t)) \exp(\omega_i t)$$

When $\omega_i < 0$, it is a damped wave. The amplitude of the wave will decay exponentially in time. When $\omega_i > 0$, the amplitude of wave grows exponentially in time and therefore unstable. Since the complex root comes with pair, as long as $\omega_i \neq 0$, one of the roots must correspond to an unstable wave. The following graph shows the two-stream instability in phase space.

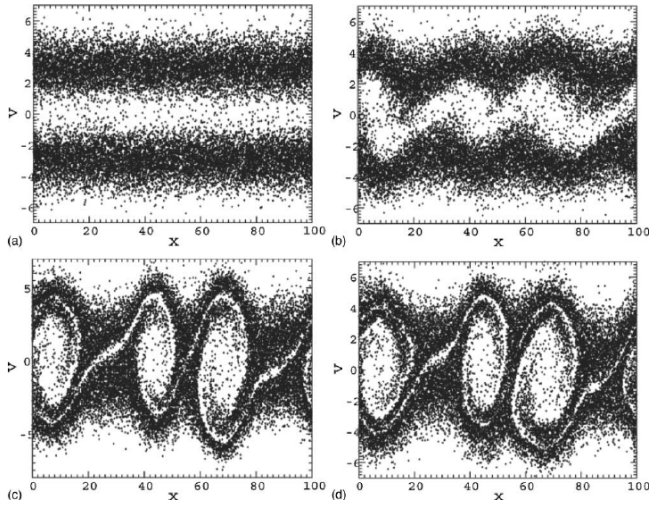

Figure 1.8: Visualization of two-stream instability in the phase space. (a) Initially the ion and electron flow are in opposite direction. (b) The velocity of both flows start to oscillate. (c) Chaotic behavior occurs. (d) The chaotic behavior continues. [4]

Overall, the study of plasma instabilities is crucial for advancing plasma physics research, optimizing plasma devices, and improving our ability to control and utilize plasmas effectively in various applications such as fusion energy, plasma propulsion, materials processing, and astrophysics.

1.4 Goals of this Thesis

The major goal of this thesis is to study the instability of plasma flow in magnetic mirror configuration with different boundary conditions.

Fluid model of plasma will be reviewed and linearized governing equations will be derived in chapter 2. The problem will be then formulated as an eigenvalue problem.

In chapter 3, spectral method and shooting method for solving eigenvalue problem will be introduced. In the section of spectral method, different discretizations of the operators, such as finite difference and spectral method will be discussed. Moreover, spectral pollution and its filtering will as also be investigated.

Then in the next section, we will formulate the problem to the form suitable for applying shooting method. We will apply both shooting method and spectral method to the problem. By comparing the results from two different methods, the credibility of the results are increased.

In chapter 5, we ill use the method developed in chapter 3 to conduct numerical experiments. The goal is to extract the eigenvalues (frequency) of each oscillating mode.

Conclusion will in chapter 6.

Chapter 2

Governing Equations

2.1 Fluid Description for Flow

In this section, we will derive the governing equations of the flow in magnetic nozzle, starting from the fluid description for plasma.

In magnetic nozzle, the magnetic field is along the nozzle, which we denote as z-axis. Due to Lorentz force, the charged particles gyrates about the magnetic field lines. Because the magnetic moment is invariant in such situation. [3] The fluid velocity of particles can be written as $\mathbf{v} = v\mathbf{B}/B$, meaning that the particles move along the magnetic field lines. Therefore the conservation of density

$$\frac{\partial n}{\partial t} + \boldsymbol{\nabla} \cdot (n\mathbf{v}) = 0 \Rightarrow \frac{\partial n}{\partial t} + B\frac{\partial}{\partial z}\Big(\frac{nv}{B}\Big) = 0$$

In the derivation, the divergence-free condition for magnetic field, $\boldsymbol{\nabla} \cdot \mathbf{B} = 0$, is used.

To derive the second governing equation, we start from the conservation of momentum,

$$\frac{\partial v}{\partial t} + v\frac{\partial v}{\partial z} = -\frac{1}{\rho}\boldsymbol{\nabla} p$$

Let $\boldsymbol{\nabla} p = k_B T\ \partial n/\partial z$, we have

$$\frac{\partial v}{\partial t} + v\frac{\partial v}{\partial z} = -c_s^2 \frac{1}{n}\frac{\partial n}{\partial z}$$

where $c_s^2 = k_B T/m$ is the square of sound speed.

Therefore the dynamics of the flow in magnetic nozzle can be characterized by the conservation of density and momentum,

$$\frac{\partial n}{\partial t} + B\frac{\partial}{\partial z}\Big(\frac{nv}{B}\Big) = 0$$
$$\frac{\partial v}{\partial t} + v\frac{\partial v}{\partial z} = -c_s^2 \frac{1}{n}\frac{\partial n}{\partial z}$$

The magnetic field profile was discussed in Sec.1.2.1.

2.2 Linearized Equations

2.2.1 Non-dimensionalization

For convenience, we nondimensionalize the governing equations by normalizing the velocity to c_s, $v \mapsto v/c_s$, z to system length L, $z \mapsto z/L$ and time $t \mapsto c_s t/L$. The governing equations become

$$\frac{\partial n}{\partial t} + n\frac{\partial v}{\partial z} + v\frac{\partial n}{\partial z} - nv\frac{\partial_z B}{B} = 0 \tag{2.1}$$

$$n\frac{\partial v}{\partial t} + nv\frac{\partial v}{\partial z} = -\frac{\partial n}{\partial z} \tag{2.2}$$

and the nondimensionalized equilibrium condition is

$$\frac{\partial}{\partial z}\Big(\frac{n_0 v_0}{B}\Big) = 0 \tag{2.3}$$

$$v_0\frac{\partial v_0}{\partial z} = -\frac{1}{n_0}\frac{\partial n_0}{\partial z} \tag{2.4}$$

2.2.2 Linearization

As illustrated in Sec.1.3.2, it is essential to linearize the governing equations in order to investigate the instability of plasma. Now we are going to derive the linearized governing equations with the equilibrium conditions given in above.

Let $n = n_0(z) + \tilde{n}(z,t)$ and $v = v_0(z) + \tilde{v}(z,t)$, where $\tilde{n}$ and $\tilde{v}$ are small perturbed quantities.

We first linearize Eq.(2.1) by setting $n = n_0 + \tilde{n}$ and $v = v_0 + \tilde{v}$,

$$\frac{\partial(n_0+\tilde{n})}{\partial t} + (n_0+\tilde{n})\frac{\partial(v_0+\tilde{v})}{\partial z} + (v_0+\tilde{v})\frac{\partial(n_0+\tilde{n})}{\partial z} - (n_0+\tilde{n})(v_0+\tilde{v})\frac{\partial_z B}{B} = 0$$

By ignoring the second order perturbations, we obtain

$$\frac{1}{n_0}\frac{\partial\tilde{n}}{\partial t} + \frac{\partial v_0}{\partial z} + \frac{\tilde{n}}{n_0}\frac{\partial v_0}{\partial z} + \frac{\partial\tilde{v}}{\partial z} + \frac{v_0}{n_0}\frac{\partial n_0}{\partial z} + \frac{\tilde{v}}{n_0}\frac{\partial n_0}{\partial z} + \frac{v_0}{n_0}\frac{\partial\tilde{n}}{\partial z} - v_0\frac{\partial_z B}{B} - \tilde{v}\frac{\partial_z B}{B} - \tilde{n}\frac{v_0}{n_0}\frac{\partial_z B}{B} = 0$$

Using the equilibrium condition Eq.(2.3), some of the terms are canceled. Moreover, the last term can be written as

$$\tilde{n}\frac{v_0}{n_0}\frac{\partial_z B}{B} = \frac{\tilde{n}}{n_0}\left(\frac{\partial_z n_0}{n_0}v_0 + \frac{\partial v_0}{\partial z}\right)$$

Now, we get the linearized conservation of mass,

$$\frac{1}{n_0}\frac{\partial\tilde{n}}{\partial t} + \frac{\partial\tilde{v}}{\partial z} + v_0\tilde{Y} + \tilde{v}\frac{\partial_z n_0}{n_0} - \tilde{v}\frac{\partial_z B}{B} = 0 \tag{2.5}$$

where

$$\tilde{Y} \equiv \frac{1}{n_0}\frac{\partial\tilde{n}}{\partial z} - \frac{\partial_z n_0}{n_0^2}\tilde{n} = \frac{\partial}{\partial z}\left(\frac{\tilde{n}}{n_0}\right)$$

To linearize the conservation of momentum, we follow the same logic by substituting $n = n_0 + \tilde{n}$, and $v = v_0 + \tilde{v}$ in Eq.(2.2),

$$(n_0 + \tilde{n})\frac{\partial(v_0 + \tilde{v})}{\partial t} + (n_0 + \tilde{n})(v_0 + \tilde{v})\frac{\partial(v_0 + \tilde{v})}{\partial z} = -\frac{\partial n}{\partial z}$$

Again, ignore second order perturbations and rearange terms, we have

$$\frac{\partial v_0}{\partial t} + v_0\frac{\partial v_0}{\partial z} + \tilde{v}\frac{\partial v_0}{\partial z} = -\frac{1}{n_0}\frac{\partial n_0}{\partial z} - \frac{1}{n_0}\frac{\partial \tilde{n}}{\partial z} - v_0\frac{v_0}{z} - \frac{\tilde{n}}{n_0}v_0\frac{\partial v_0}{\partial z}$$

Using the equilibrium condition Eq.(2.4) on the RHS, we get the linearized conservation of momentum,

$$\frac{\partial \tilde{v}}{\partial t} + \frac{\partial(v_0\tilde{v})}{\partial z} = -\tilde{Y} \tag{2.6}$$

2.3 Polynomial Eigenvalue Problem

We can further simplify the problem by combining Eq.(2.5) and Eq.(2.6) into a single equation. We can substitute Eq.(2.6) into Eq.(2.5) to eliminate $\tilde{Y}$,

$$\frac{\partial}{\partial t}\frac{\tilde{n}}{n_0} + \frac{\partial \tilde{v}}{\partial z} - v_0\left(\frac{\partial}{\partial t}\tilde{v} + \frac{\partial(v_0\tilde{v})}{\partial z}\right) + \tilde{v}\frac{\partial_z n_0}{n_0} - \tilde{v}\frac{\partial_z B}{B} = 0 \tag{2.7}$$

In order to investigate the instability of the flow, we need formulate it as an eigenvalue problem. To do that, we assume the perturbed density and velocity are oscillatory, i.e. $\tilde{n}, \tilde{v} \sim \exp(-i\omega t)$, where ω is the oscillation frequency of the perturbed quantities. This frequency can be a complex number.

As illustrated in Sec.1.3.2, the flow can be stable or unstable depending on the imaginary part of the frequency. If $\mathrm{Im}(\omega) > 0$, then the perturbed quantities $\tilde{n} \sim \exp(\mathrm{Im}(\omega)t)$, which means it grows exponentially with time, hence unstable. If $\mathrm{Im}(\omega) \leq 0$, then the amplitude of the perturbed quanties are either unchanged or exponentially decreasing, hence the flow is stable.

By assuming oscillatory perturbed quantities, Eq.(2.7) becomes,

$$-i\omega\frac{\tilde{n}}{n_0} + \frac{\partial \tilde{v}}{\partial z} - v_0\left(-i\omega\tilde{v} + \frac{\partial(v_0\tilde{v})}{\partial z}\right) + \tilde{v}\frac{\partial_z n_0}{n_0} - \tilde{v}\frac{\partial_z B}{B} = 0 \tag{2.8}$$

Using the equilibrium condition Eq.(2.3), we can eliminate the term $\partial_z B/B$,

$$-i\omega\frac{\tilde{n}}{n_0} + \frac{\partial \tilde{v}}{\partial z} + v_0\left(i\omega\tilde{v} - v_0\frac{\partial \tilde{v}}{\partial z} - \tilde{v}\frac{\partial v_0}{\partial z}\right) - \tilde{v}\frac{\partial_z v_0}{v_0} = 0$$

Rearrange terms, we have

$$-i\omega\frac{\tilde{n}}{n_0} + i\omega v_0\tilde{v} + (1 - v_0^2)\frac{\partial \tilde{v}}{\partial z} - \left(v_0 + \frac{1}{v_0}\right)\frac{\partial v_0}{\partial z}\tilde{v} = 0$$

Now we take $\partial/\partial t$ on Eq.(2.6). Recall the fact that $\tilde{Y} = \partial_z(\tilde{n}/n_0)$, we have

$$\omega^2\tilde{v} + i\omega\left(v_0\frac{\partial\tilde{v}}{\partial z} + \tilde{v}\frac{\partial v_0}{\partial z}\right) = \frac{\partial}{\partial t}\frac{\partial}{\partial z}\left(\frac{\tilde{n}}{n_0}\right)$$

Apply ∂_t operator first, we get

$$\omega^2\tilde{v} + i\omega\left(v_0\frac{\partial\tilde{v}}{\partial z} + \tilde{v}\frac{\partial v_0}{\partial fz}\right) = \frac{\partial}{\partial z}\left(-i\omega v_0\tilde{v} - (1-v_0^2)\frac{\partial\tilde{v}}{\partial z} + \left(v_0 + \frac{1}{v_0}\right)\frac{\partial v_0}{\partial z}\tilde{v}\right)$$

Expand the RHS and collect terms, we get

$$\begin{aligned}
&\omega^2\tilde{v} \\
&+ 2i\omega\left(v_0\frac{\partial}{\partial z} + \frac{\partial v_0}{\partial z}\right)\tilde{v} \\
&+ \left[(1-v_0^2)\frac{\partial^2}{\partial z^2} - \left(3v_0 + \frac{1}{v_0}\right)\frac{\partial v_0}{\partial z}\frac{\partial}{\partial z} - \left(1 - \frac{1}{v_0^2}\right)\left(\frac{\partial v_0}{\partial z}\right)^2 - \left(v_0 + \frac{1}{v_0}\right)\frac{\partial^2 v_0}{\partial z^2}\right]\tilde{v} = 0
\end{aligned} \tag{2.9}$$

Eq.(2.9) is an polynomial eigenvalue problem. In Chap.(3) we will discuss the methods to tackle this problem.

Chapter 3

Methodology

3.1 Spectral Method

Spectral method is one of the best tools to solve PDE and ODE problems. [8] The central idea of spectral method is by discretizing the equation, we can transform that to a linear system or an eigenvalue problem.

Here we reformulate the polynomial eigenvalue problem, Eq.(2.9) as the following,

$$\begin{bmatrix} 0 & 1 \\ \hat{M} & \hat{N} \end{bmatrix} \begin{bmatrix} \tilde{v} \\ \omega\tilde{v} \end{bmatrix} = \omega \begin{bmatrix} \tilde{v} \\ \omega\tilde{v} \end{bmatrix} \tag{3.1}$$

where the operators $\hat{M}$ and $\hat{N}$ are defined as

$$\hat{M} = -\left[(1 - v_0^2)\frac{\partial^2}{\partial z^2} - \left(3v_0 + \frac{1}{v_0}\right)\frac{\partial v_0}{\partial z}\frac{\partial}{\partial z} - \left(1 - \frac{1}{v_0^2}\right)\left(\frac{\partial v_0}{\partial z}\right)^2 - \left(v_0 + \frac{1}{v_0}\right)\frac{\partial^2 v_0}{\partial z^2} \right]$$

$$\hat{N} = -2i\left(v_0\frac{\partial}{\partial z} + \frac{\partial v_0}{\partial z}\right)$$

This becomes an ordinary algebraic eigenvalue problem if we discretize the operators and the function $\tilde{v}$. The following subsections discuss different discretizations of the problem.

3.1.1 Finite Difference

Consider equally spaced nodes on domain $[-1, 1]$, $\{x_1, x_2, \ldots, x_N\}$ with $x_{j+1} - x_j = h$ for each j, and the set of corresponding function values, $\{f_1, f_2, \ldots, f_N\}$. We can approximate the derivatives using second-order central difference formulas

$$\frac{\partial f}{\partial z} = \frac{f_{j+1} - f_{j-1}}{2h} \qquad \frac{\partial^2 f}{\partial z^2} = \frac{f_{j+1} - 2f_j + f_{j-1}}{h^2}$$

We can discretize the differentiation operators to the following matrices

$$\frac{\partial}{\partial z} \to D = \frac{1}{2h}\begin{bmatrix} 0 & 1 & 0 & \dots & 0 \\ -1 & \ddots & \ddots & \ddots & \vdots \\ 0 & \ddots & \ddots & \ddots & 0 \\ \vdots & \ddots & \ddots & \ddots & 1 \\ 0 & \dots & 0 & -1 & 0 \end{bmatrix} \qquad \frac{\partial^2}{\partial z^2} \to D^2 = \frac{1}{h^2}\begin{bmatrix} -2 & 1 & 0 & \dots & 0 \\ 1 & \ddots & \ddots & \ddots & \vdots \\ 0 & \ddots & \ddots & \ddots & 0 \\ \vdots & \ddots & \ddots & \ddots & 1 \\ 0 & \dots & 0 & 1 & -2 \end{bmatrix}$$

Using these differentiation matrices, Eq.(3.1) becomes

$$\begin{bmatrix} O & I \\ M & N \end{bmatrix}\begin{bmatrix} \tilde{\mathbf{v}} \\ \omega\tilde{\mathbf{v}} \end{bmatrix} = \omega\begin{bmatrix} \tilde{\mathbf{v}} \\ \omega\tilde{\mathbf{v}} \end{bmatrix} \tag{3.2}$$

where O is a zero matrix, I is an identity matrix, and

$$\begin{aligned} M =& -\operatorname{diag}(1-\mathbf{v}_0^2)D^2 + \operatorname{diag}\left(3\mathbf{v}_0 + \frac{1}{\mathbf{v}_0}\right)(D\mathbf{v}_0)D + \operatorname{diag}\left(1 - \frac{1}{\mathbf{v}_0^2}\right)(D\mathbf{v}_0)^2 \\ &+ \operatorname{diag}\left(\mathbf{v}_0 + \frac{1}{\mathbf{v}_0}\right)(D^2\mathbf{v}_0) \\ N =& -2i\left(\operatorname{diag}(\mathbf{v}_0)D + D\mathbf{v}_0\right) \end{aligned}$$

Here we abused the notation for the purpose of convenience, $\mathbf{v}_0^2$ means squaring every component of $\mathbf{v}_0$, and $1/\mathbf{v}_0$ denotes 1 divided by all components of $\mathbf{v}_0$.

Boundary Condition

We impose Dirichlet boundary condition on the problem, meaning that $\tilde{v}(-1) = \tilde{v}(1) = 0$. Further more, the differentiation matrices do not do well on the edges, so during the computation, we remove the first and last row of the differentiation matrices and the vectors $\tilde{\mathbf{v}}$ and $\mathbf{v}_0$. After the computation, we set $\tilde{v}_1 = \tilde{v}_N = 0$.

3.1.2 Spectral Element

Suppose the basis functions are $\{u_k(z)\}_{k=1}^{\infty}$, then the eigenfunction $\tilde{v}$ can be approximated by finite amount of them, $\tilde{v}(z) = \sum_{k=1}^{N} c_k u_k(z)$ where c_k are coefficients to be determined.

Then by multiplying u_i to any term and integrate through the domain, we can discretize the equation. Using the notation of inner product $(f, g) = \int_{-1}^{1} dz f g$, we see that

$$\int_{-1}^{1} dz\; u_i \tilde{v} = \sum_j (u_i, u_j) c_j$$

$$\int_{-1}^{1} dz\; u_i \frac{\partial \tilde{v}}{\partial z} = \sum_j \left(u_i, \frac{\partial u_j}{\partial z}\right) c_j$$

$$\int_{-1}^{1} dz\ u_i \frac{\partial^2 \tilde{v}}{\partial z^2} = \sum_j \left(u_i, \frac{\partial^2 u_j}{\partial z^2} \right) c_j$$

Suppose the basis functions are $\{u_k(z)\}_{k=1}^{\infty}$, then the eigenfunction $\tilde{v}$ can be approximated by finite amount of them, $\tilde{v}(z) = \sum_{k=1}^{N} c_k u_k(z)$ where c_k are coefficients to be determined.

$$\begin{bmatrix} O & I \\ M & N \end{bmatrix} \begin{bmatrix} \mathbf{c} \\ \omega \mathbf{c} \end{bmatrix} = \omega \begin{bmatrix} \mathbf{c} \\ \omega \mathbf{c} \end{bmatrix} \tag{3.3}$$

where O is a zero matrix, I is an identity matrix, and

$$M_{jk} = -\int_{-1}^{1} dz\ u_j \left[(1 - v_0^2) \frac{\partial^2}{\partial z^2} - \left(3v_0 + \frac{1}{v_0} \right) \frac{\partial v_0}{\partial z} \frac{\partial}{\partial z} - \left(1 - \frac{1}{v_0^2} \right) \left(\frac{\partial v_0}{\partial z} \right)^2 - \left(v_0 + \frac{1}{v_0} \right) \frac{\partial^2 v_0}{\partial z^2} \right] u_k$$

$$N_{jk} = -2i \int_{-1}^{1} dz\ u_j \left(v_0 \frac{\partial}{\partial z} + \frac{\partial v_0}{\partial z} \right) u_k$$

Boundary Conditions and Basis Function

To satisfy the Dirichlet boundary condition, $\tilde{v}(\pm 1) = 0$, we can choose a set of basis functions that satisfy the boundary condition $u_k(\pm 1) = 0, \forall k \in \mathbb{N}$. For example, the sine functions

$$u_n(z) = \sin\Big(\frac{n\pi}{2}(z+1) \Big), n \in \mathbb{N}$$

is a set of basis functions that satisfy the Dirichlet boundary condition.

3.1.3 Finite Element

Finite-element method is a generalization of the spectral element method. We are allow to use a set of basis functions similar to spectral method in a cell. The region consists of many of these cells.

The formulation is the same as Eq.(3.3). The only difference is that in finite-element we need to solve Eq.(3.3) simultaneously for all cells.

Boundary Conditions and B-Spline

The B-Spline is a commonly used basis function for finite-element method. B-Spline can be defined recursively starting with piecewise constants [reference needed]

$$B_{i,0}(\xi) = \begin{cases} 1, & \text{if } \xi_i \le \xi \le \xi_{i+1} \\ 0, & \text{otherwise} \end{cases} \tag{3.4}$$

For $j \in \mathbb{N}$, they are defined by

$$B_{i,j}(\xi) = \frac{\xi - \xi_i}{\xi_{i+j} - \xi_i} B_{i,j-1}(\xi) + \frac{\xi_{i+j+1} - \xi}{\xi_{i+j+1} - \xi_{i+1}} B_{i+1,p-1}(\xi) \tag{3.5}$$

where $\xi = [\xi_0, \cdots, \xi_m]$ is called the knot vector, where $m = n + j + 1$ where $n + 1$ is the number of B-Splines and j is the degree of B-Spline polynomials. The knot vector defines the shapes of the B-Splines, see Fig.3.1. The variable ξ is within the range $[\xi_0, \xi_m]$.

Any function $u(x)$ on $[\xi_0, \xi_N]$ can be approximated by

$$u(x) \simeq \sum_{j=0}^{n} c_j B_{i,j}(x)$$

The Dirichlet boundary condition can be set by letting the coefficients of the first and last B-Spline to 0, $c_0 = c_n = 0$, where N is the number of B-Splines.

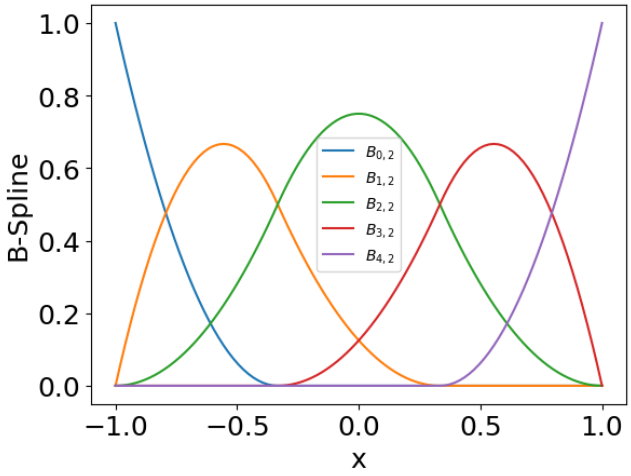

Figure 3.1: An example of open uniform quadratic B-Spline on $[-1, 1]$. The knot vector is $[-1, -1, -1, -1/3, 1/3, 1, 1, 1]$.

3.2 Shooting Method

Shooting method can be used to solve eigenvalue problem with specified boundary values,

$$g(\tilde{v}(z); \omega) = 0, \quad z_l \leq z \leq z_r, \quad \tilde{v}(z_l) = \tilde{v}_l, \tilde{v}(z_r) = \tilde{v}_r \tag{3.6}$$

where ω is the eigenvalue to be solved.

Suppose a eigenvalue problem can be formulated as

$$\frac{\mathrm{d}}{\mathrm{d}z}\mathbf{u} = \mathbf{f}(\mathbf{u}, z; \omega), \quad z_l < z < z_r, \quad \mathbf{u}(z_l) = \mathbf{u}_l$$

where $\mathbf{u} \in \mathbb{R}^2$. Fixed an ω, we can approximate $\mathbf{u}(z_r)$ by applying algorithms such as Runge-Kutta or Leap-frog.

Define F by $F(\mathbf{u}_l;\omega) = \tilde{v}(z_r;\omega)$. This function F takes in the initial value $\mathbf{u}_l$ and a fixed ω, and outputs the "landing point" $\tilde{v}(z_r;\omega)$. If ω is an eigenvalue of Eq.(3.6), then $\tilde{v}(z_r;\omega) = \tilde{v}_r$. Now we can find eigenvalues to Eq.(3.6) by solving the roots to the scalar equation

$$h(\omega) = F(\mathbf{u}_l;\omega) - \tilde{v}_r$$

Having this higher view of shooting method in mind, we first transform Eq.(2.9) to a IVP,

$$v' = u$$

$$u' = \frac{-1}{1-v_0^2}\left[\omega^2 v + 2i\omega(v_0 + v_0' v) - \left(3v_0 - \frac{1}{v_0}\right)v_0' u - \left(1 - \frac{1}{v_0}^2\right)(v_0')^2 v - \left(v_0 + \frac{1}{v_0}v_0'' v\right)\right]$$

and $v(0) = c_0 = 1, u(0) = c_1 = (2i\omega v_0' - 2v_0'')/2v_0'$. Moreover, $u'(0) = c_2 = -((v_0')^4 + (2i\omega v_0' + (v_0')^2 - v_0'')(i\omega v_0' - v_0''))/(v_0'(2i\omega - 6v_0'))$.

In order to get initially value for cases with transonic velocity profiles, we need to expand the solution at the singularity.

3.2.1 Expansion at Singularity

If the equilibrium velocity profile v_0 is a transonic profile, then $v_0(0) = 1$ at the throat of the magnetic mirror configuration. This is a singularity. More specifically, it is a regular singular point.

In order to supply initial values to shooting method, we need to expand Eq.(2.9) at the singularity.

Since

$$\begin{aligned} 1 - v_0^2 &= -2v_0'(0)z \\ 3v_0 + \frac{1}{v_0} &= 4 + 2v_0'(0)z \\ 1 - \frac{1}{v_0^2} &= 2v_0'(0)z \\ v_0 + \frac{1}{v_0} &= 2 \end{aligned} \tag{3.7}$$

Then Eq.(2.9) becomes

$$\begin{aligned} &-2v_0'(0)z\frac{\partial^2\tilde{v}}{\partial z^2} \\ &+[2i\omega - 4v_0'(0) + (2i\omega - 2v_0'(0))z]\frac{\partial\tilde{v}}{\partial z} \\ &+\left[\omega^2 + 2i\omega v_0'(0) - 2v_0''(0) - 2v_0'(0)^3 z\right]\tilde{v} = 0 \end{aligned} \tag{3.8}$$

Since we are expanding at $z = 0$, we drop all z terms except the first term (second-order derivative term).

$$-2v_0'(0)z\frac{\partial^2\tilde{v}}{\partial z^2} + (2i\omega - 4v_0'(0))\frac{\partial\tilde{v}}{\partial z} + (\omega^2 + 2i\omega v_0'(0) - 2v_0''(0))\tilde{v} = 0$$

Dividing by the first coefficient, we have

$$z\frac{\partial^2\tilde{v}}{\partial z^2} + a\frac{\partial\tilde{v}}{\partial z} + b\tilde{v} = 0 \tag{3.9}$$

where

$$a = \frac{2i\omega - 4v_0'(0)}{-2v_0'(0)}; \quad b = \frac{\omega^2 + 2i\omega v_0'(0) - 2v_0''(0)}{-2v_0'(0)}$$

Use Frobenius method, we assume $\tilde{v} = \sum_{n\geq 0} c_n z^{n+r}$, plug Eq.(3.9) we have

$$\sum_{n\geq 0}(n+r)(n+r+1)c_n z^{n+r-1} + a(n+r)c_n z^{n+r-1} + bc_n z^{n+r} = 0$$

Shift the power of the last term we get

$$\sum_{n\geq 0}(n+r)(n+r+1)c_n z^{n+r-1} + a(n+r)c_n z^{n+r-1} + \sum_{n\geq 1} bc_{n-1} z^{n+r-1} = 0$$

Setting $n = 0$, we get the indicial equation

$$c_0 r(r-1) + c_0 ar = 0 \Rightarrow c_0 r(r+a-1) = 0$$

We get two different roots, $r = 0$ and $r = 1 - a$. They correspond to finite solution and diverging solution near the singularity, respectively.

The coefficients are given by reccurence relation

$$(n+r)(n+r-1)c_n + a(n+r)c_n + bc_{n-1} = 0 \Rightarrow c_n = \frac{-bc_{n-1}}{(n+r)(n+r-1+a)}$$

Solving this relation we get explicit expression for c_n,

$$\begin{aligned} c_n &= \frac{(-1)^n b^n c_0}{\prod_{k=0}^{n-1}(n+r-k)(n+r-1+a-k)} \\ &= (-1)^n b^n c_0 \frac{\Gamma(r+1)\Gamma(r+a)}{\Gamma(n+r+1)\Gamma(n+r+a)} \end{aligned} \tag{3.10}$$

- Worth to mention that the diverging solution goes like

  $$\tilde{v}(z) \sim z^{1-a} = z^{-1-\omega_i/v_0'(0)} z^{i\omega_r/v_0'(0)}$$

  where $\omega = \omega_r + i\omega_i$. Meaning that the solution will be divergent iff $\omega_i > -v'(0)$.

- Droping the z terms in Eq.(3.8) has no effect on the first order correction ($\tilde{v}$ is the same up to z term).

Chapter 4

Theoretical Analysis

4.1 Constant Velocity

4.1.1 Dirichlet Boundary

If we set the velocity profile of the equilibrium flow to constant $v_0 = \text{const}$, then Eq.(2.9) becomes a simple boundary value problem with second order constant coefficients differential equation.

$$\omega^2\tilde{v} + 2i\omega v_0\frac{\partial\tilde{v}}{\partial z} + (1 - v_0^2)\frac{\partial^2\tilde{v}}{\partial z^2} = 0 \quad \tilde{v}(-1) = \tilde{v}(1) = 0 \tag{4.1}$$

The solution to this problem is

$$\tilde{v} = C\left[\exp\left(i\omega\frac{z+1}{v_0+1}\right) - \exp\left(i\omega\frac{z+1}{v_0-1}\right)\right] \tag{4.2}$$

where $C \in \mathbb{C}$ is a complex constant, and the frequencies are $\omega = n\pi(1 - v_0^2)/2$ with $n \in \mathbb{Z}$.

This result tells us for constant velocity case, the flow in magnetic nozzle is stable regardless the velocity v_0. It is worth to mention $v_0 = 1$ is a singular point of this problem.

We will use this to benchmark the simulation results.

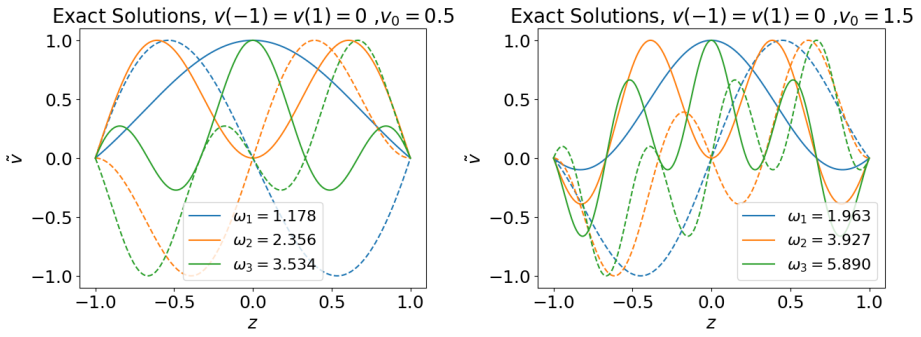

(a) Subsonic (b) Supersonic

Figure 4.1: The plots show the first three non-zero exact solutions to Eq.(4.1) for both subsonic and supersonic case. These solutions are stable.

4.1.2 Fixed-Open Boundary

$$\omega^2\tilde{v} + 2i\omega v_0\frac{\partial\tilde{v}}{\partial z} + (1-v_0^2)\frac{\partial^2\tilde{v}}{\partial z^2} = 0 \quad \tilde{v}(-1) = \frac{\partial\tilde{v}}{\partial z}(1) = 0 \tag{4.3}$$

The solution to this problem is

$$\tilde{v} = C\left[\exp\left(i\omega\frac{z+1}{v_0+1}\right) - \exp\left(i\omega\frac{z+1}{v_0-1}\right)\right] \tag{4.4}$$

where $C \in \mathbb{C}$, and $\omega = (v_0^2-1)\left[\frac{n\pi}{2} - \frac{1}{4}i\ln\left(\frac{v_0-1}{v_0+1}\right)\right]$ with $n \in \mathbb{Z}$. For any $v_0 \neq 1$, the term $i\ln((v_0-1)/(v_0+1)) \in \mathbb{C}$ and its imaginary part is positive. Therefore,

- If $v_0 < 1$, then $\mathrm{Im}(\omega) < 0$, it's damped oscillation, hence stable.
- If $v_0 > 1$, then $\mathrm{Im}(\omega) > 0$, it's unstable.

Worth to mention, this is a very interesting solution with the following properties,

1. The growth rate is independent the mode number n.
2. The ground mode $n = 0$ for subsonic case has non-zero real part and imaginary part.

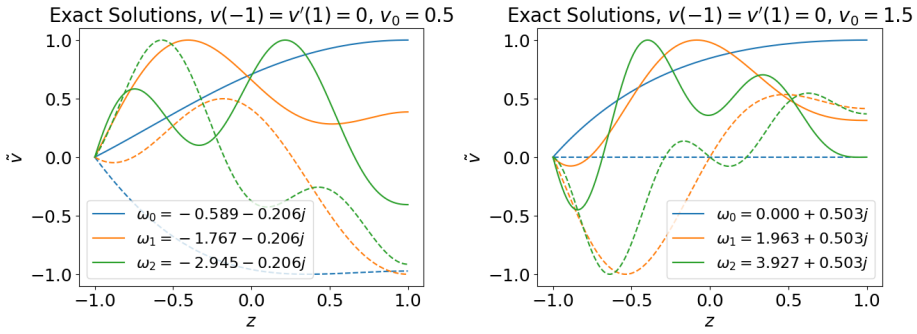

(a) Subsonic, stable flow.

(b) Supersonic, unstable flow.

Figure 4.2: The plots show the first three exact solutions to Eq.(4.3) for both subsonic and supersonic case. The flow is stable for subsonic case and unstable for supersonic case.

4.2 Spectral Pollution and Spurious Modes

In this section, we will discuss an important phenomenon we observe throughout the numerical experiments. It is the phenomenon of spectral pollution. Then we will provide a method to filter these spurious modes.

Spectral pollution refers to the phenomenon which some eigenvalues are not converging to the correct value when the mesh density is increased. When solving eigenvalue problems using spectral methods with finite difference or finite element approximations, spectral pollution might occur. [7]

4.2.1 Finite Difference Discretization of Operators

In this section, we are going to investigate the spectral pollution phenomenon when solving Eq.(4.1) using spectral method.

The dispersion relation can be obtained by substituting $\tilde{v} = \exp(-i\omega t + kx)$ into Eq.(4.1),

$$\omega = k(v_0 \pm 1) \tag{4.5}$$

If we assume $v \sim \exp(ikx)$, and let $\beta \equiv kh/2$. Then in finite difference discretization scheme, the differential operators $\mathrm{d}^n/\mathrm{d}z^n$ are equivalent to the following factors [7],

$$\begin{aligned} G_0 &= 1 \\ G_1 &= [\exp(2i\beta) - \exp(-2i\beta)]/2h = (i/h)\sin(2\beta) \\ G_2 &= [\exp(2i\beta) - 2 - \exp(-2i\beta)]/h^2 = (2/h^2)(\cos(2\beta) - 1) \end{aligned} \tag{4.6}$$

4.2.2 Analysis of Numerical Spectrum

Discretize on the Same Grid

Using the G-operator, Eq.(4.6), the discretized equation of Eq.(4.1) is

$$(\omega^2 G_0 + \omega G_1 + G_2)\tilde{\mathbf{v}} = 0 \tag{4.7}$$

where $\tilde{\mathbf{v}}$ is the discretized vector of $\tilde{v}$.

Solving Eq.(4.7), we obtain the numerical dispersion relation,

$$\omega = \frac{2\sin(\beta)}{h}\left(v_0 \pm \sqrt{1 - v_0^2 \sin^2(\beta)}\right) \tag{4.8}$$

Given h (fixed the mesh resolution), we see that

- ω is real for all k if $v_0 < 1$.
- ω is complex for large k, more specifically $k > h/2 \arcsin(1/v_0)$, if $v_0 > 1$.
- For small k, meaning $k \to 0$, Eq.(4.8) is a good representation for the analytical dispersion relation, Eq.(4.5).

This explains why the spurious unstable modes occur when $v_0 > 1$.

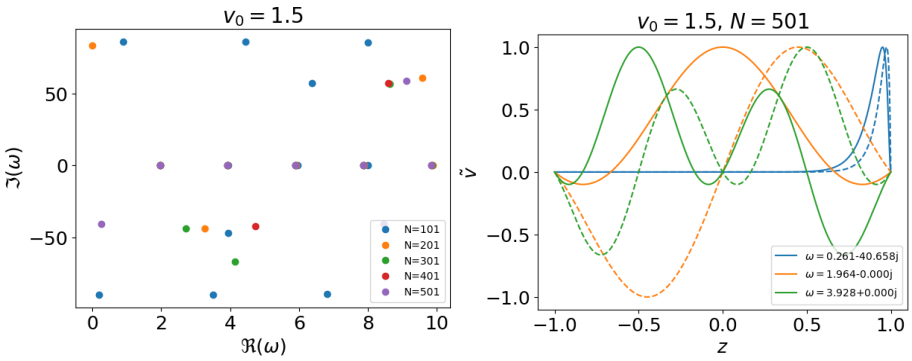

(a) Bad eigenvalues

(b) Bad eigenfunctions

Figure 4.3: Spurious modes.

One way to filter the spurious modes is to remove all modes with $k > h/2 \arcsin(1/v_0)$, see Fig.**??**. However, this is not a good way to deal with general cases because it requires the solution to the discretized problem Eq.(4.7). For general problem with non-constant velocity profile, it is hard to solve the discretized problem directly.

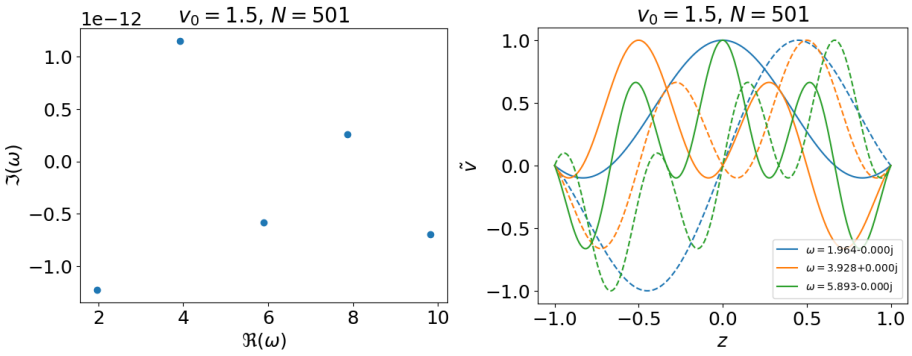

(a) Good eigenvalues

(b) Good eigenfunctions

Figure 4.4: Filter out the spurious modes with $k > h/2 \arcsin(1/v_0)$.

A better way to filter the spurious modes is by doing a "convergence test". Since the frequency Eq.(4.8) is changing with mesh resolution h. We can simply solve the discretized problem using spectral method under different mesh resolution. Then filter out the eigenmodes that are changing dramatically.

Chapter 5

Numerical Experiments

In this chapter, we will solve the eigenvalue problem, Eq.(3.1), with different discretizations. There will be three major categories of methods used. Finite difference (FD) method, finite element (FE) method and spectral element method (SE).

The finite difference method will be used together with equally spaced nodes. The finite element method will use B-spline as basis functions. Finally, the spectral element method uses sine functions as the spectral elements.

For Dirichlet boundary, The parameters of different discretizations are listed below

Table 5.1: With Dirichlet boundary condition, all methods have good accuracy, so using 101 nodes in the region $[0, 1]$ is enough. For FE and SE methods, they are using 50 basis functions.

	FD	FE_BSPLINE	SE_SINE
N	101	101	101
NUM_BASIS		51	50

For left-fixed and right-open (fixed-open) boundary condition, the parameters are

Table 5.2: With fixed-open boundary condition, it requires higher resolution in order to get accurate results. Therefore all methods use 501 nodes in the region $[0, 1]$, and FE method uses 101 basis functions.

	FD	FE_BSPLINE
N	501	501
NUM_BASIS		101

5.1 Constant Velocity Case

5.1.1 Dirichlet Boundary

Because the existence of exact solution to problems Eq.(4.1). The case with constant velocity profile is used as a sanity check. It allows us to verify the correctness of each method's implementation. This also serves as a reference to the accuracy spectral methods can achieve.

From Fig.(**??**), we see that the order of growth rates obtained by different methods is about 10^{-14} for both subsonic and supersonic cases. We will use these numbers as a reference to the accuracy of our numerical methods. If a method produces growth rates with order close to 10^{-14}, we consider the growth rates to be 0.

Table 5.3: Relative error of each eigenvalue.

$v_0 = 0.5$	1	2	3	4	5
FD	2.827e-05	1.130e-04	2.541e-04	4.512e-04	7.040e-04
FE	0.005	0.005	0.006	0.008	0.010
SE	2.896e-05	1.157e-04	2.603e-04	4.626e-04	7.217e-04

$v_0 = 1.5$	1	2	3	4	5
FD	0.001	0.005	0.010	0.019	0.030
FE	0.006	0.010	0.019	0.029	0.043
SE	0.001	0.005	0.011	0.019	0.030

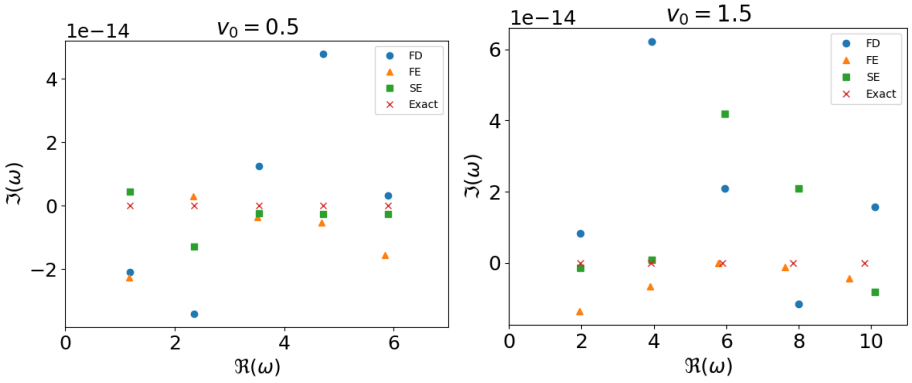

(a) All modes are stable.

(b) Filtered modes are stable.

Figure 5.1: Showing the first 5 eigenvalues of each method in each case. All methods are close to the exact eigenvalues.

5.1.2 Fixed-Open Boundary

Table 5.4: Relative error of each eigenvalue. Notice that the ground mode for subsonic case is non-zero.

$v_0 = 0.5$	0	1	2	3	4
FD	1.209e-05	3.458e-05	5.775e-05	8.153e-05	1.061e-04
FE	8.090e-05	2.007e-04	2.981e-04	6.596e-04	1.821e-03
$v_0 = 1.5$	1	2	3	4	5
FD	9.163e-05	2.435e-04	4.833e-04	8.160e-04	1.243e-03
FE	4.431e-04	7.924e-04	1.516e-03	3.103e-03	8.001e-03

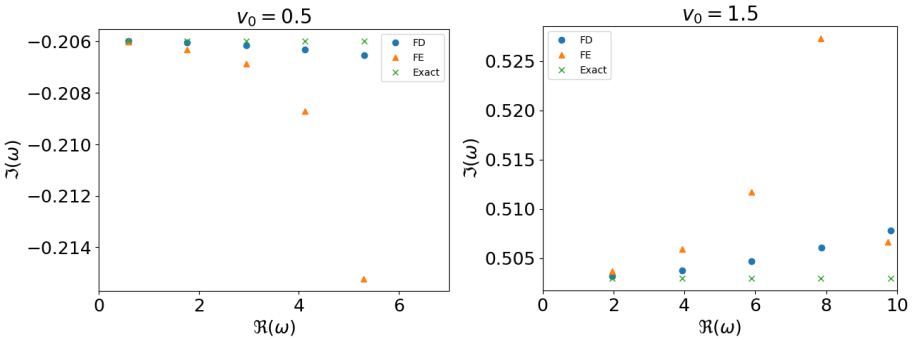

(a) All modes are stable.

(b) All modes are unstable.

Figure 5.2: Showing the first 5 eigenvalues of each method. Finite-difference method has much better accuracy than finite-element method.

5.2 Subsonic Case

5.2.1 Dirichlet Boundary

When setting the mid-point velocity to be $M_m = 0.5$, we have the subsonic velocity profile. This velocity profile is the orange line shown in Fig.1.5. With Dirichlet boundary condition, $\tilde{v}(\pm 1) = 0$. The flow in magnetic nozzle is stable. Fig.5.3 shows the first few eigenvalues obtained by different discretizations.

The order of growth rates obtained by different methods is 10^{-13}, we can consider it to be stable.

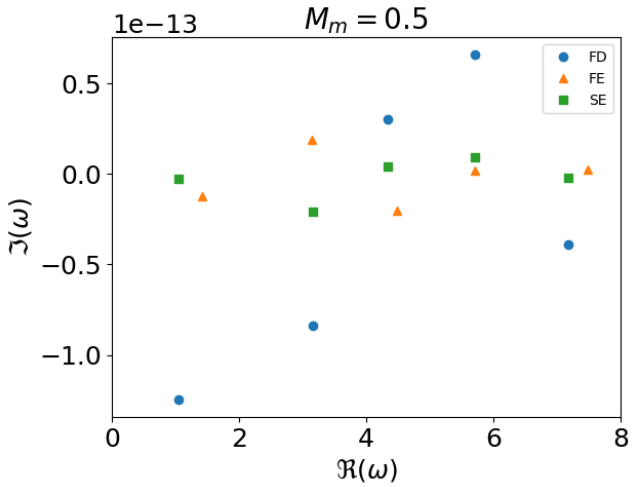

Figure 5.3: Showing the first 5 modes. It suggests that the flow in magnetic nozzle with subsonic velocity profile and Dirichlet boundary condition is stable.

5.2.2 Fixed-Open Boundary

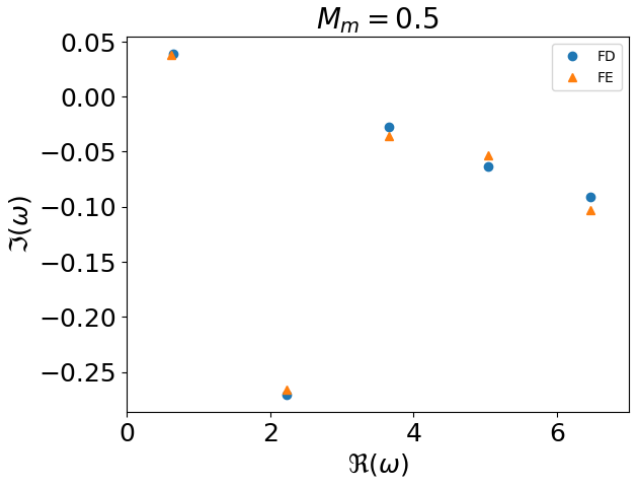

Figure 5.4: Showing the first 5 modes. The ground mode is unstable, other modes are stable.

5.3 Supersonic Case

5.3.1 Dirichlet Boundary

When the velocity profile is supersonic, shown as purple line in Fig.1.5, spurious modes appeared as predicted in Chap.4. Using the convergence test, we successfully eliminates all unstable modes. Fig.(5.5) shows the first few filtered eigenvalues. As we can see the flow is stable.

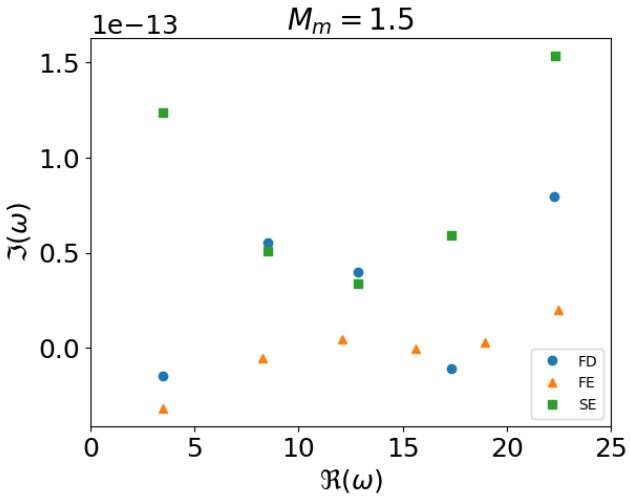

Figure 5.5: First few filtered eigenvalues are shown. The spurious modes are filtered by convergence test.

5.3.2 Fixed-Open Boundary

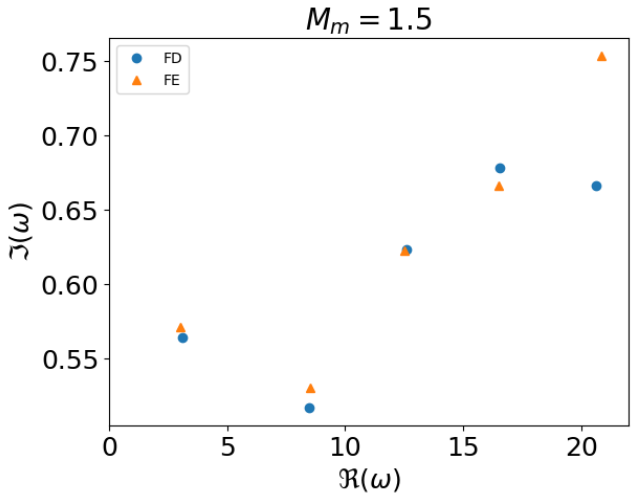

Figure 5.6: All modes are unstable.

5.4 Accelerating Case

Starting from the singular point, we shoot the solution to the left boundary. We find the set of eigenvalues such that $\tilde{v}(-1) = 0$. With these eigenvalues, we can extend the solution to the supersonic region $(0, 1]$. The first five eigenvalues are drawn in the graph.

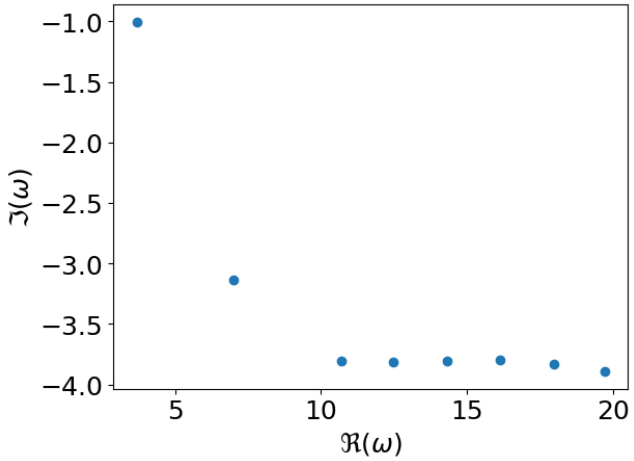

Figure 5.7: first five modes are stable.

Chapter 6

conclusion

In chapter 3, we derived the linearized equations of motion of the flow in one dimensional magnetic nozzle. Furthermore, we rewrite the linearized governing equations as an eigenvalue problem. Using the spectral methods introduced in chapter 2, we discretized the operators of the problem. Hence transforming it into an algebraic eigenvalue problem.

With the aid of computer, we are able to solve the algebraic eigenvalue problem. The results show that the flow in magnetic nozzle with Dirichlet boundary condition is stable except the case with decelerating velocity profile.

Bibliography

[1] Toshiki Aikawa. The stability of spherically symmetric accretion flows. *Astrophys Space Sci*, 66(2):277–285, December 1979.

[2] H. Bondi. On Spherically Symmetrical Accretion. *Monthly Notices of the Royal Astronomical Society*, 112(2):195–204, April 1952.

[3] Francis F. Chen. *Introduction to Plasma Physics and Controlled Fusion*. Springer International Publishing, Cham, 2016.

[4] Seung-Yeal Ha, Taeyoung Ha, Chi-Ok Hwang, and Ho Lee. Nonlinear instability of the one-dimensional Vlasov-Yukawa system. *Journal of Mathematical Physics*, 52(3):033301, March 2011.

[5] Eric Keto. Stability and solution of the time-dependent Bondi–Parker flow. *Monthly Notices of the Royal Astronomical Society*, 493(2):2834–2840, April 2020.

[6] Justin M Little. Performance scaling of magnetic nozzles for electric propulsion, 2015. ISBN: 9781321565317.

[7] X. Llobet, K. Appert, A. Bondeson, and J. Vaclavik. On spectral pollution. *Computer Physics Communications*, 59(2):199–216, June 1990.

[8] Lloyd N Trefethen. *Spectral Methods in Matlab*.

Appendix

Lambert W function

Verification of analytical solutions

Theorem 1. The general solution to

$$\omega^2\tilde{v} + 2i\omega\frac{\partial\tilde{v}}{\partial z} + (1-v_0^2)\frac{\partial^2\tilde{v}}{\partial z^2} = 0$$

is

$$\tilde{v} = \exp\left(-\frac{i\omega}{v_0+1}\right)\left[\exp\left(i\omega\frac{z+1}{v_0+1}\right) - \exp\left(i\omega\frac{z+1}{v_0-1}\right)\right]$$

Proof. The derivatives of $\tilde{v}$ are

$$\begin{aligned}
\tilde{v} &= \exp\left(-\frac{i\omega}{v_0+1}\right)\left[\exp\left(i\omega\frac{z+1}{v_0+1}\right) - \exp\left(i\omega\frac{z+1}{v_0-1}\right)\right] \\
\frac{\partial\tilde{v}}{\partial z} &= i\omega\exp\left(-\frac{i\omega}{v_0+1}\right)\left[\frac{1}{v_0+1}\exp\left(i\omega\frac{z+1}{v_0+1}\right) - \frac{1}{v_0-1}\exp\left(i\omega\frac{z+1}{v_0-1}\right)\right] \\
\frac{\partial^2\tilde{v}}{\partial z^2} &= -\omega^2\exp\left(-\frac{i\omega}{v_0+1}\right)\left[\frac{1}{(v_0+1)^2}\exp\left(i\omega\frac{z+1}{v_0+1}\right) - \frac{1}{(v_0-1)^2}\exp\left(i\omega\frac{z+1}{v_0-1}\right)\right]
\end{aligned}$$

Then the rest is easy,

$$\begin{aligned}
&\omega^2\tilde{v} + 2i\omega\frac{\partial\tilde{v}}{\partial z} + (1-v_0^2)\frac{\partial^2\tilde{v}}{\partial z^2} \\
=&\exp\left(-\frac{i\omega}{v_0+1}\right)\left(1 - \frac{2v_0}{v_0+1} + \frac{(1-v_0^2)}{(v_0+1)^2}\right)\exp\left(i\omega\frac{z+1}{v_0+1}\right) \\
&-\exp\left(-\frac{i\omega}{v_0+1}\right)\left(1 - \frac{2v_0}{v_0-1} + \frac{(1-v_0^2)}{(v_0-1)^2}\right)\exp\left(i\omega\frac{z+1}{v_0-1}\right) \\
=&0
\end{aligned}$$

□

Theorem 2. If $\omega = n\pi(1 - v_0^2)/2$, then $\tilde{v}(\pm 1) = 0$.

Proof. It is easy to see that $v(-1) = 0$. As for $z = 1$, we have

$$\begin{aligned}
\tilde{v}(1) &\propto \exp\left(\frac{2i\omega}{v_0 + 1}\right) - \exp\left(\frac{2i\omega}{v_0 - 1}\right) \\
&= \exp(in\pi(1 - v_0)) - \exp(-in\pi(1 + v_0)) \\
&= (-1)^n \exp(-in\pi v_0) - (-1)^n \exp(-in\pi v_0) \\
&= 0
\end{aligned}$$

□

Theorem 3. If

$$\omega = (v_0^2 - 1)\left[\frac{n\pi}{2} - \frac{1}{4} i \ln\left(\frac{v_0 - 1}{v_0 + 1}\right)\right]$$

then $\tilde{v}(-1) = 0$ and $\partial_z \tilde{v}(1) = 0$.

Proof. It is easy to see that $v(-1) = 0$. The derivative at $z = 1$ is

$$\begin{aligned}
\left.\frac{\partial \tilde{v}}{\partial z}\right|_{z=1} \propto & \frac{1}{v_0 + 1} \exp\left(\frac{2i\omega}{v_0 + 1}\right) - \frac{1}{v_0 - 1} \exp\left(\frac{2i\omega}{v_0 - 1}\right) \\
= & \frac{1}{v_0 + 1} \exp\left(in\pi(v_0 - 1) + \frac{v_0 - 1}{2} \ln\left(\frac{v_0 - 1}{v_0 + 1}\right)\right) \\
& - \frac{1}{v_0 - 1} \exp\left(in\pi(v_0 + 1) + \frac{v_0 + 1}{2} \ln\left(\frac{v_0 - 1}{v_0 + 1}\right)\right) \\
= & \frac{(-1)^n}{v_0 + 1} \exp(in\pi v_0) \left(\frac{v_0 - 1}{v_0 + 1}\right)^{(v_0 - 1)/2} \\
& - \frac{(-1)^n}{v_0 - 1} \exp(in\pi v_0) \left(\frac{v_0 - 1}{v_0 + 1}\right)^{(v_0 + 1)/2} \\
= & 0
\end{aligned}$$

The last equality holds because

$$\frac{1}{v_0 - 1} \left(\frac{v_0 - 1}{v_0 + 1}\right)^{(v_0 + 1)/2} = \frac{1}{v_0 + 1} \left(\frac{v_0 - 1}{v_0 + 1}\right)^{(v_0 - 1)/2}$$

□